A Review on Common Approaches Used for Graphene Characterization

Omar S. Dahham[1*], Khalid Al-Zamili[2], Nik Noriman Zulkepli[3]

[1]Department of Chemical Engineering, College of Engineering, University of Baghdad, Baghdad, Iraq.
[2]Department of Oil and Gas Refinery Engineering, Al-Farabi University College, Baghdad, Iraq.
[3]Faculty of Mechanical Engineering Technology, Universiti Malaysia Perlis, Perlis, Malaysia.

*Corresponding E-mail: omar.s@coeng.uobaghdad.edu.iq

Abstract

Graphene particularly one layer of carbon atoms in 2D crystal lattice of honeycomb has gain much attention because of its distinctive electronic and optoelectronic properties. The stated characteristics of this material with a unique structure of carbon that in turn opened-up new aspects for the future systems and devices. Despite the graphene is a unique electronic material, synthesizing graphene with a single layer was less investigated. Thus, it is important to cover the main methods used for characterizing the graphene such as Raman, TEM, SEM AFM, XRD and UV-Vis with a view to the fundamental principles of each method.

Keywords: *Graphene, Graphite, Characterization, Morphology, Raman Spectroscopy.*

1. Introduction

Graphene commonly describes as the wonder material of the 21st century while the polymer was the wonder material in the 20th century. Graphene is obtained from graphite and it is simply a single graphite sheet. This single sheet consists of only one atom of sp_2 hybridized atoms of carbon prearranged in a structure of honeycomb with unique features such as good chemical stability, high surface area and excellent electrical conductivity [1–4]. The expedition of the graphene has started in the year 2007, when Konstantin Novoselov and Andre K. Geim (Noble laureates) have discovered the huge potential of graphene in different applications by observing its electrical characteristics. Also stated that "Graphene is the highflier on the horizon of materials science and condensed matter physics", in their research study about graphene [1]. Graphene begun developing every sector from energy, health to environment [5–8]. Its mechanical, optical, and electrical properties [9–11] are outstanding that makes graphene an extremely desirable material for numerous application.

Some applications emphasize; graphene is glowing as wavelength wide range used because of its varied electronic structure. High mobility and optical transparency are graphene characteristics that are the optoelectronic devices requirements. Currently graphene became a good ITO replacement.

Graphene acts a vital role in optic-based-devices like the convertors of optical frequency, terahertz devices and flexible-smart-windows into a next level. Furthermore, the graphene optical absorption might be altered by regulating the Fermi level. Graphene was also currently recognized as a multi-faceted nano-material for biomedical purposes. It also uses for biological purposes from to neural interface, drug delivery to cell scaffolds. Graphene could also be in ultra-filtration field that has started the development because of its morphology of 2D shape that contain a relatively high surface

area. Besides it is classified as the best membrane for applications of water treatment. Ultra-thin shape of graphene has attracted the attentions of the researchers and engineers to apply it in water purification processes [12]. It has huge potential for treatment of wastewater.

Further it is considered as the best substitute material that is employed for treatment photocatalysis that plays as a scavenger of electrons. Thus, improving the catalyst efficiency. Thus graphene is being investigated for biological application [13], flexible display [14], memory devices [15], supercapacitor [16], ultra-fast transistor [17], light emitting diode [18], fuel cell [19], solar cell [20], water treatment [21] and battery [22], In every research conducted, the scientists are capable to achieve a valuable outcomes.

3. Characterization of Graphene

Synthesized graphene can be described via different approaches of characterization. **Raman** is an imperative spectroscopy equipment utilized for investigating the structure of the graphene. The transmission-electron-microscope (**TEM**) is also a significant analysis for distinguishing the graphene structure (i.e: no of graphene layers) because of its capability to analyze the level of graphene atom. The **SEM** and **AFM** were widely utilized to illustrate the graphene morphology. Other less important analyses such as **XRD** and **UV-Vis**, were also utilized as a supportive test for the findings.

3.1 Raman spectroscopy

Raman is a nondestructive spectroscopy device utilized for characterizing the graphene film. The carbon allotropes illustrate distinctive characteristic peaks in Ramanspectroscopy at around 1345, 1575 and 2690 cm^{-1}[23,24]. These peaks help scientists and the researchers to study the graphene quality as well as the layers number of the graphene produced. The D band refers to the sp^2-hybridized atoms disorder of carbon and is distinguishing of lattice distortions, while the G band refers to the mode of tangential peak (E_{2g}) of pyrolytic graphite (highly oriented). The 2D band refers to the Raman scattering process (second order) [25-27]. Few investigations were observed on the synthesis of graphene by a chemical reduction rout includes a defects with higher density compared with synthesis of graphene by chemical vapor deposition and other routes [28]. Figure 1. (a) illustrates the spectra of Raman of graphite/graphene, and the outstanding characteristics of graphene appeared at the three peaks of D, G and 2D at $1350cm^{-1}$, 1580 and 2680 respectively. Generally, graphite and graphene revealed clear differences in level of their peaks (G, D, and 2D), as exhibited in Figure 1. (a). Furthermore, the graphene quality can be investigated from the Raman spectrum via ratio calculation of the intensities for 2D/G (I_{2D}/I_G). A large I_{2D}/I_G ratio and a comparatively small intensity of D peak demonstrates that a graphene high quality was formed [24, 29]· In Figure 1. (b), graphene that is produced via chemical vapor deposition demonstrates a higher I_{2D}/I_G ratio than grapheme synthesized by mechanical exfoliation. Consequently, chemical vapor deposition is considered as the most proper techniques can be used to produce graphene high quality. Furthermore, the small peak of D shows that high quality of graphene sheets were successfully synthesized, as shown in Fig. 32-b [30].

Yoon et al reported an easy method to detect and calculate the number of layers for graphene produced as shown in Figure 9. [24], this figure shows a comparison among the 2D intensities of G* and G band for different graphene layers numbers. In the G band, it can be detected that the intensity has increased as the layers number increase up to 7 layers and while it has decreased for the higher thickness of graphene layer Figure 2a. Thus, the variation in the G band intensity presents some clue on the graphene layers

number [24]. The G* band has a comparatively less intensity than the 2D and G bands, this is obviously shown that the band of G* place is slightly moved from 2445 to 2455 cm–^{1} and the graphene layers number increased. Moreover, the band of G* of single layer graphene shown in Figure. 2. (b) is sharper than multi-layer graphene. Besides, the band of 2D for graphene can be utilized to differentiate the single-layer from the graphene multi layers of [24]. The graphene with single layer reveals a greater and sharper intensity 2D peak than other peaks Figure 2 (c)). Ferrari et al. have also distinguished single-, double- and multi graphene layers effectively by using Raman spectroscopy [31].

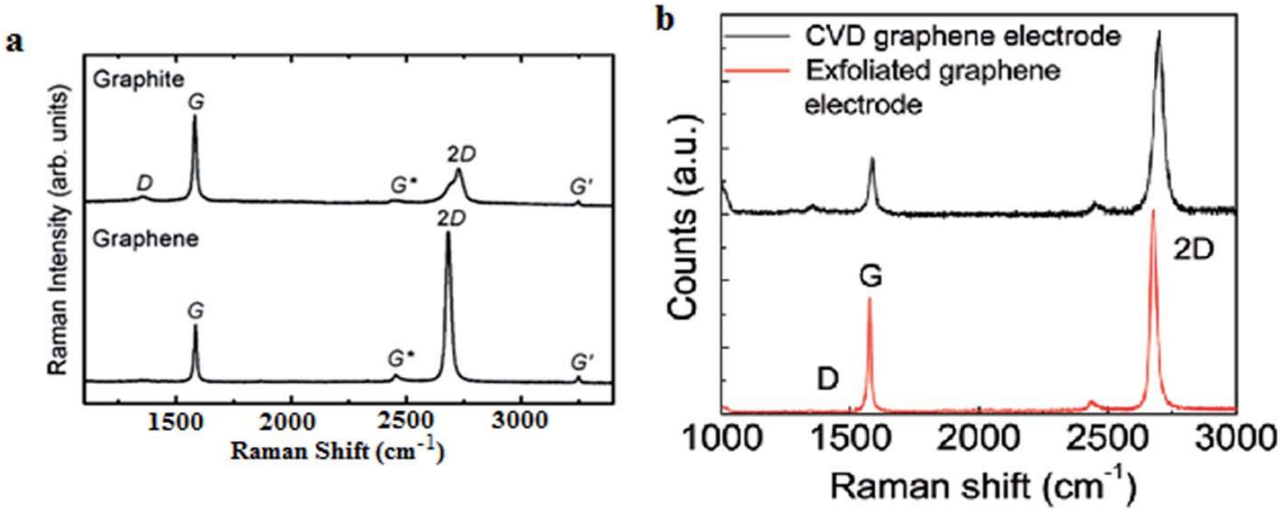

Fig 1. (a) Spectra of Raman of graphene and graphite.

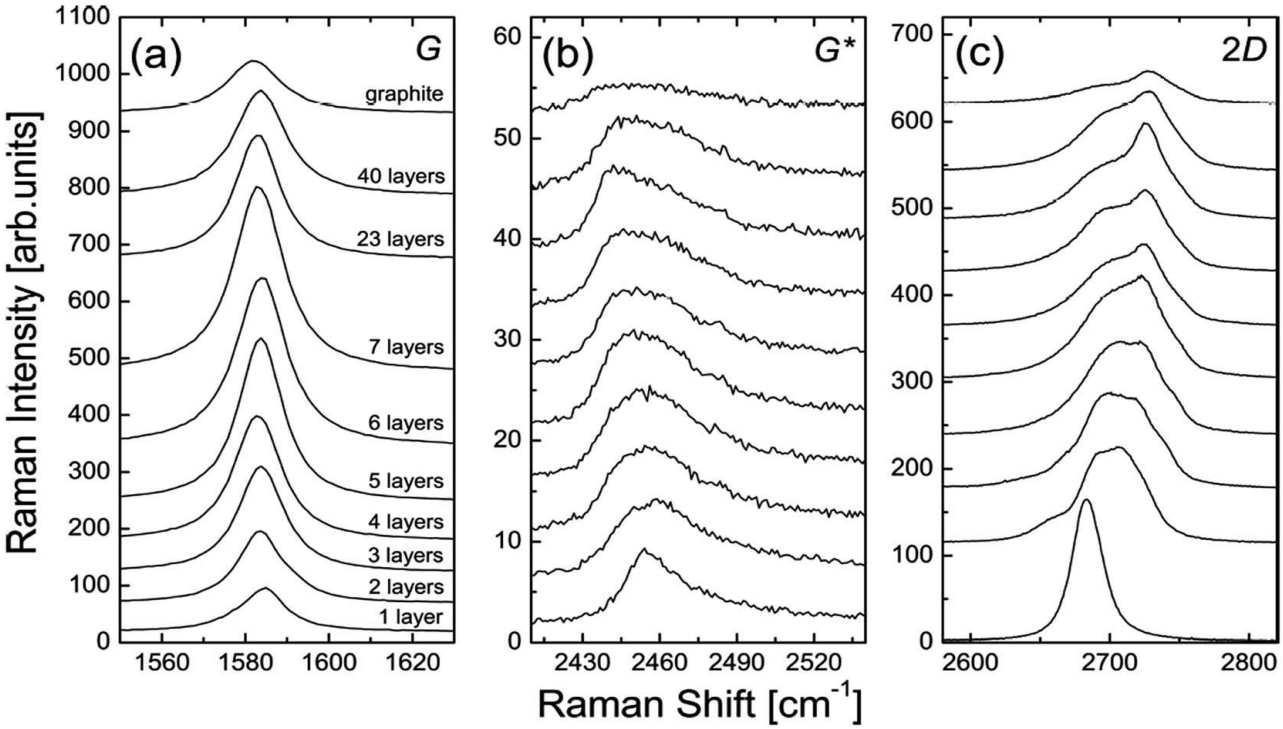

Fig 2. Variation of the band of: (a) G, (b) G*, and (c) 2 D using spectra of Raman.

3.2 TEM

TEM utilize high voltage electrons for transition throughout an extremely thin layer of sample. After the sample is places, the obtained reflected-signal is converted to an image to investigate the morphological

variations of the sample(s) [32]. Thus, the very thin sample is essential in TEM analysis. Graphene characterization using TEM is an essential analysis due to its ability to image graphene in a nano or even in an atomic level;[36] for example, for dislocations, vacancy, Stone–Wales rotation, point defects, and many more [37]. Graphene with a single-layer is commonly acts as a transparent as TEM applied. The high/low TEM micrographs magnification of a graphene (single layer) converted to a TEM grid as shown in Figure 3 (a) and (b), respectively, with the related pattern of SAED (inset) [38]. A graphene with single layer is successfully spotted in the TEM micrographs, as shown in Figure 10 (b), while the pattern of SAED (inset in Figure 3(b)) shows the hexagonal shape of graphene in crystalline form. Furthermore, few layers graphene can be obviously observed in the TEM images as shown in Figure 4. a to Figure 4 f. The patterns of SAED illustrated in Figure 4(g)–(i) are uneven, and the double, three, and five layers graphene are not be to justify according to these patterns. Hence, other characterization, particularly spectroscopy of Raman, is essential to support the findings of TEM analysis.

Figure 5 (a). Reveals the TEM images of graphene synthesized by using alcohol (ethanol) as a foundation of carbon via the chemical vapor deposition method. The graphene sheet was well fabricated on the scale of microscopic. Figure 5(b) and (d) show the bent edges of the single and double layers of graphene correspondingly that enable the number of layers of the graphene to be calculated. Moreover, the analysis of SAED in the micrographs demonstrats that the graphene formed were poly-crystalline [39].

Also, graphene with single-layer film can be produced via zeolite as both the catalyst and template. Figure 13. displays the TEM micrograph of the produced graphene film, whereas the image displays the graphene with single layer only. Under TEM observation, it can be obviously observed that the graphene sheet is interlaced and transparent. Besides, it is found that the produced graphene nanosheet was ultrathin and flat [40].

In order to analyze the graphene crystallinity, SAED patterns have been recognized from 6 different graphene sample areas as shown in Figure 7(a). Figure 7(b). displays the graphene-cracked site. Figure 7c. exhibits the presence of graphene with singlelayer only. As observed in Figure 7(d), all the examined 6 places shown as a single crystalline graphene because there is an only one shape of hexagonal spots of diffraction without any rotation observed. Consequently, the whole region of the graphene as labeled from 1 to 6 in Figure 7(a) includes a singlecrystalline graphene [41].

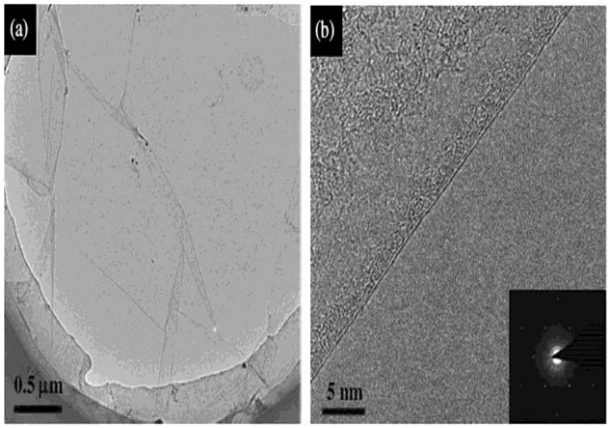

Fig 3. TEM micrograph of graphene with single layer at magnification (a) Low / (b) high.

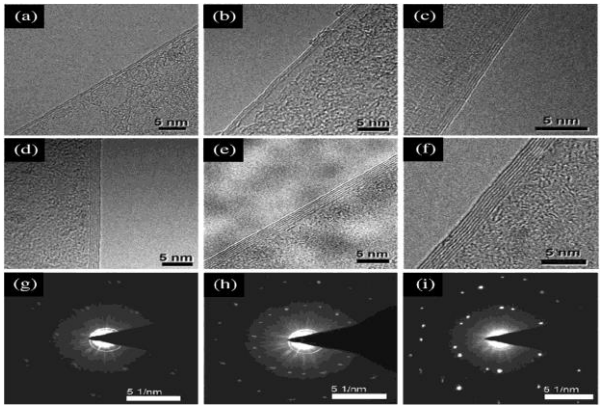

Fig 4. Micrographs of TEM of the graphene edges at different layers numbers: (a) 2 layers, (b) 3 layers, (c) 4 layers, (d) 5 layers, (e) 6 layers and (f) 7 layers. The patterns of SAED of 2, 3 and 5 layers of graphene obtained from the domains center are presented from (g) to (i).

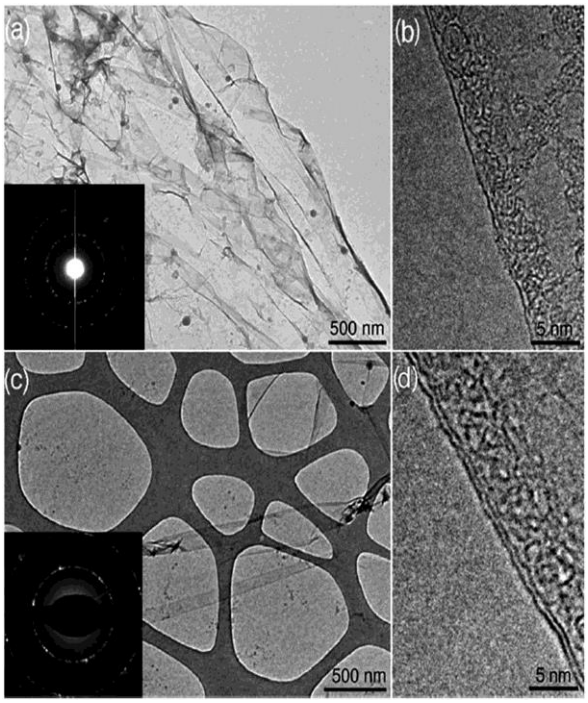

Fig 5. TEM micrograph of graphene sheets transmitted to grids of TEM (a) graphene sheet grown for 20 seconds at temp 1000 C (b) single layer graphene fold. (c) Sheet formed for 1 minutes at temp 1070 C (d) double layer graphene fold.

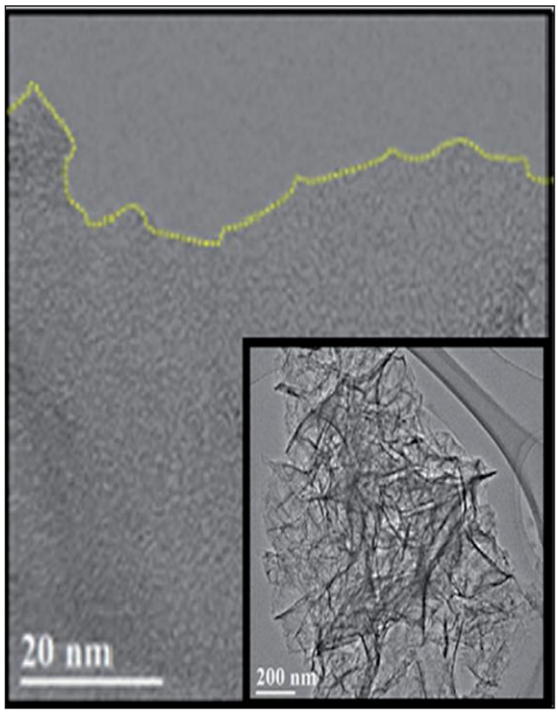

Fig 6. TEM micrograph of the aggregated graphene

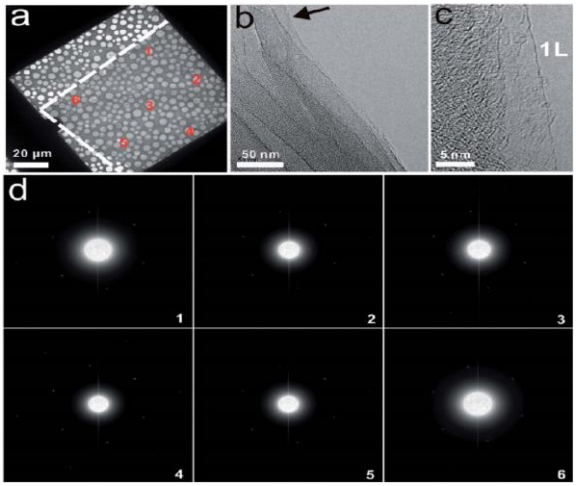

Fig 7. (a) TEM micrograph of graphene formed on grid of TEM (High-resolution). (b) TEM micrograph of a graphene cracked area. (c) TEM micrograph obtained from the area labeled with the point in b (high-resolution). (d) SAED of the 6 zones labeled at a.

3.3 SEM and FESEM

SEM and FESEM techniques are widely applied to observe the changes of morphology of graphene. The optical and electron microscope has normally similar principals of operation. Nevertheless, the electron microscope (EM) is usually used in highly energetic electrons as the source rather than the visible light that are used in the optical microscope [42]. The common microscope (optical) has a low-resolution with low magnification because the visible light has long wavelength of source used, while the accelerated electrons contain shorter wavelength than visible light wavelength, this makes SEM or FESEM in a very high resolution [43].

Cao, and Zhang, have formed the graphene from natural flake graphite via Hummers' technique using liquid oxidization, 2-dimensional graphene sheet, which examined by SEM. Also, the fold structure was observed on the edge of both surfaces of the specimen Figure 8. this is considered as typical morphologies of multi- layer graphene [14]. The thickness of the specimen was about 10 nm and it is clearly that the layers of the sample have large dimension (larger than 100 nm).

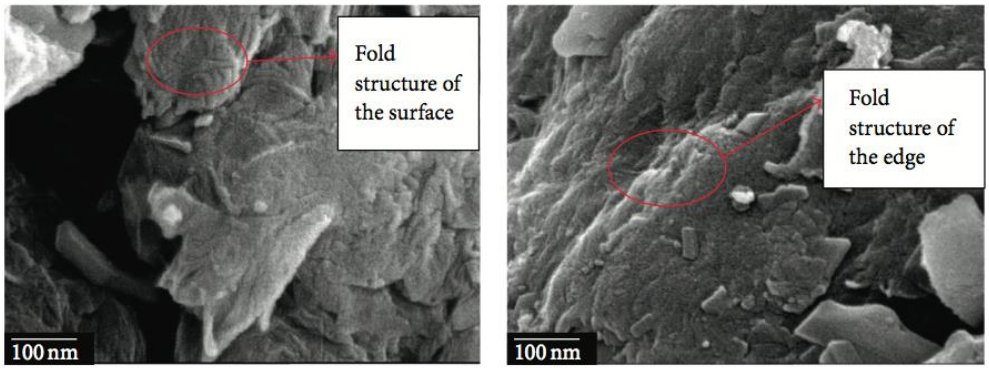

Fig 8: SEM micrograph of synthesized graphene.

Khai et al,. have formed mono and multi-layer graphene using a technique called microwave-assisted solvo-thermal and the prepared graphene was analyzed by FESEM Figure 9(a) and (b)) [44]. The prepared graphene dimensions were about of 3 - 10 mm. In Figure 9(c) and (d), single layer graphene films can be obviously observed at high and even moderate magnifications of the FE-SEM micrographs. Besides, surface crumples sheet and folded at the ends of surfaces of the graphene films as observed clearly. In contrast, the graphene (multi- layer) have also formed by Gui's et al,.[45] using the same technique “solvo-thermal”, agglomerations and wrinkles was observed that is corresponded with the research conducted by Khai et al. [44]. The existence of remaining oxygen that contains functionalgroups, comprising hydroxyl groups (–OH) and carboxyl groups (–COOH), attached on the graphene sides could be the result of the wrinkles presence [44].

Hawaldar et al. synthesized graphene film via hot filament thermal chemical vapor-deposition approach and then observed the morphological properties of the prepared sheets using FESEM (Figure 10(a)) [145]. Few wrinkles on the graphene surface seen on the substrate. Figure 10(b) represents the high- magnification of FESEM micrograph for two-layer graphene on a copper grid. another chemical vapor deposition process used for graphene synthesis, Dang et al,.[46] found that the graphene surface area can be increased as the graphene growth-time increase, which is observed from graphene assessment and times-of-growth of 10/15 minutes (Figure. 10(c) and (d)).

Figure 11. illustrates graphene produced by chemical vapor deposition method (microwave-plasma) (G1 label), and graphene produced by chemical method (G2 label) [47] The G1 graphene on the surface contained few surface folds of the sample, while G2 graphene on the surface is well deposited on the surface. In contrast, graphene produced by the chemical method was deposited unevenly. Consequently, agglomerations on the both surface were clearly observed. FESEM usually exhibits high resolution micrographs with low electrostatically distorted, which is considered as an efficient method to investigate the morphology of the graphene specimens. Furthermore, the graphene characterization using SEM is a common technique because of the low cost of SEM as compared with FE-SEM and its capability to inspect the images with reasonable magnification. Some researchers inspected the surface of formed graphene via chemical vapor deposition as shown in Figure. 12 [38]. Typically, continuous graphene was observed in spite of there being a white-folds places on the sample surface, as shown in the SEM micrographs.

SEM was also utilized to examine the growth of graphene (in situ) in a segregation method of carbon, as reported by Takahashi et al,.[48] multi layers graphene were produced using different conditions of growth, as illustrated

in Figure 13(a). the multi layers graphene are observed as darker contrast at the other side of the micrograph. While double layer graphene appeared an intermediate contrast, and the single layer graphene is seen as a brighter contrast. The contrast variation appeared in the SEM micrographs was due to the different valence electrons numbers between graphite and Nikkle (Ni) surface [49], When the graphene sample cooled down up to temperature 25 C, the distinction however was enhanced Figure 13. (b). after exposing air to the specimen, the contrast of the different graphene layers is significantly changed because of the oxidation process occurred on the surface of Nickle. Nevertheless, the Ni surface hidden under graphene sheet didn't oxidize Figure. 40(c) [50].

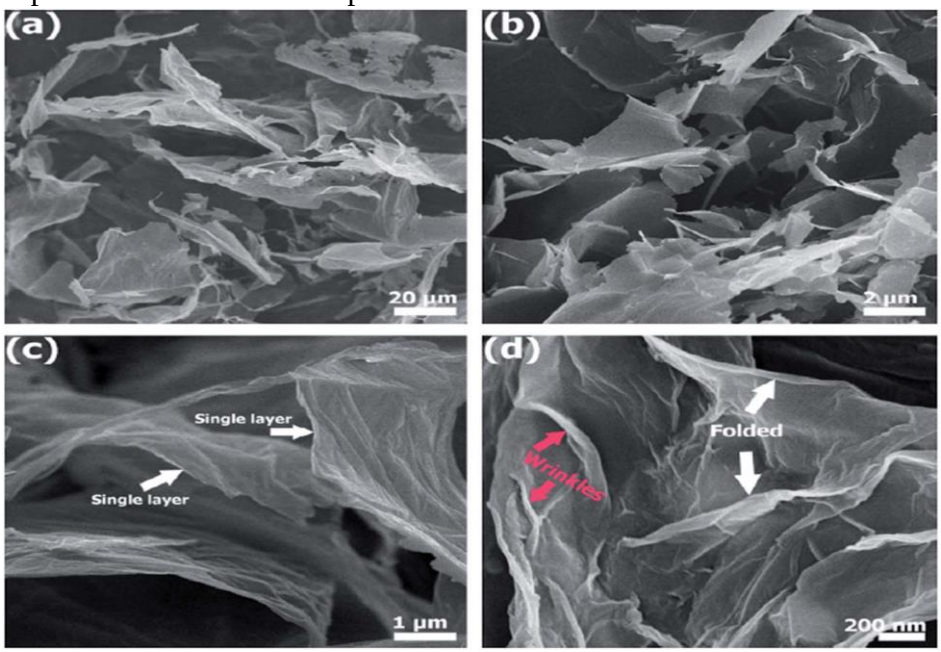

Fig 9. (a) FESEM micrographs of multi-layer graphene at magnification (a) Low, (b and c) normal, and (d) high.

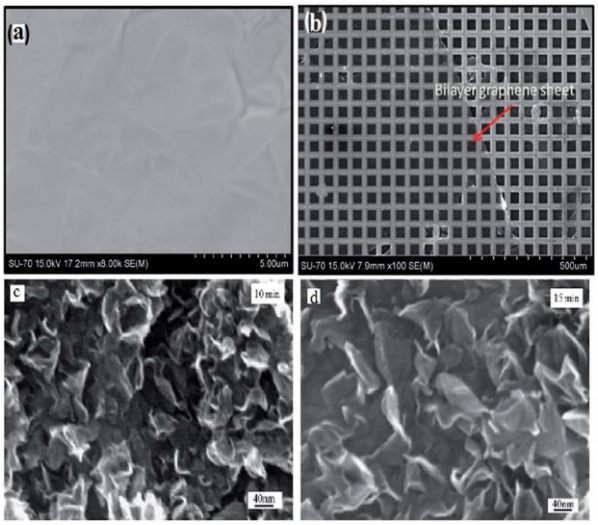

Fig 10. (a) FE-SEM image of graphene formed on copper, (b) FE-SEM image of a graphene sheet (two layers) carried on a substrate of copper, formed by thermal chemical vapour deposition (hot filament) FE-SEM images of graphene at (c) 10 minutes and (d) 15 minutes times of growth.

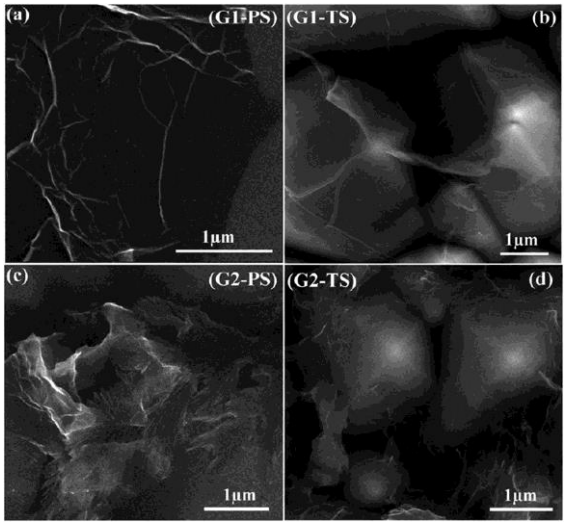

Fig 11. FESEM micrograph of graphene on substrate of: (a) polished-Silica and (b) textured-Silica, formed graphene sheet (spin-coated) on: (c) Silica polished (polished) and (d) Silica (textured).

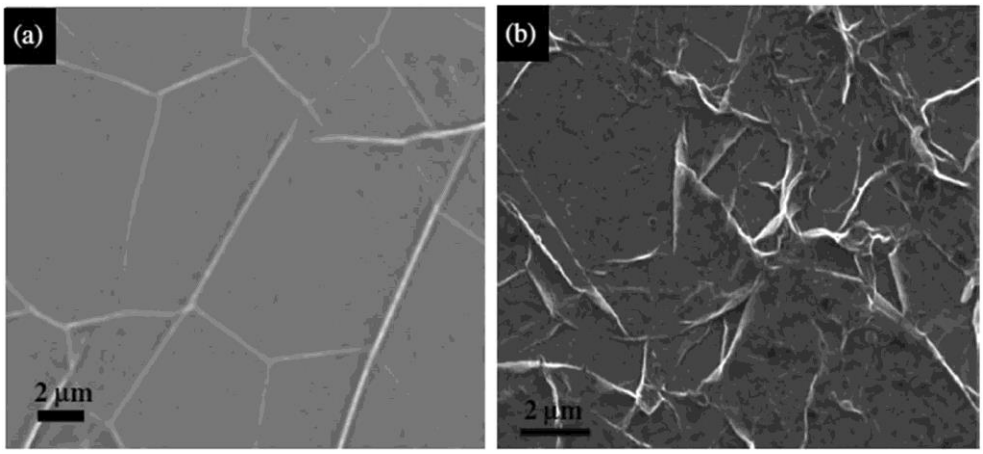

Fig 12. (a) SEM images of a graphene on multi-layers of substrate of (a) Cupper, and (b) Silica.

Fig 13. SEM micrographs displaying the different contrast for different graphene layers numbers on polycrystalline Ni Surface at: (a) an high temperature, (b) room temperature before air exposure, and (c) 25 C after air exposure.

3.4 AFM

AFM can be generally employed for characterizing the graphene with dimensions in the range of nano-meter with different states, such as ultra-high vacuum, liquids, and normal atmosphere [51]. A sharp tip of the AFM in nano-meter size is formed by micro-technology is associated with the cantilever free edge that is considered as a transducer for sensing the specimen tip [52]. Chen et al., synthesized graphene using improved Hummers method, and then analized the prepared graphene using AFM tapping mode. The sample thickness was calculated to be about 0.8 nm Figure. 14., indicating that it has a single-layer structure.

You et al. [53] have also used AFM analysis to study the roughness of the surface and also to calculate the graphene thickness. Figure 15. displays the graphene produced via technique of chemical-vapor-deposition on four different surfaces. The four samples were examined using tapping-mode of AFM. It is found that there is a direct correlation between the reaction time and the graphene surface roughness; the long processing time usually increase both thickness and roughness surface of graphene.

Gao et al. have synthesized graphene on substratum of palladium via segregation technique of surface [54]. The thickness/surface topography of the graphene sheet was studies via AFM analysis Figure. 16. It can be observed the uniform shape of graphene sheet that is entirely covered the surface of palladium, as exhibited in Figure 16(a) and (b). However, there was few nanowires of carbon were spotted on graphene top because of the growing of Carbon (3D). The specimen edge reveals the graphene discontinuity, while the surface area of the uncovered palladium and graphene can be observed clearly in Figure 16(c). The line profile thickness Figure. 52(c) has been calculated to be around 0.40 nanometer, which is agreed with the hypothetical calculation of the single layer graphene.

AFM is an efficient approach used to validate the layer thickness of graphene. Liu's et al., [55] have synthesized multi-layer graphene by conducting exfoliation technique on the expandable graphite in super-critical N,N- di-methyl-formamide solvent. Figure 17(a) and (b) illustrate the layers of graphene via tapping-method (AFM). It can be clearly observed that the sizes and thicknesses are changed, whereas most of graphene sheets were around 3 nm. In contrast, Figure 17(c) and (d) reveal the structure micrographs of the graphene (exfoliated) sample. The exfoliated graphene sample height is approximately 1.2 nm. This suggests the sample must be considered as monolayer graphene.

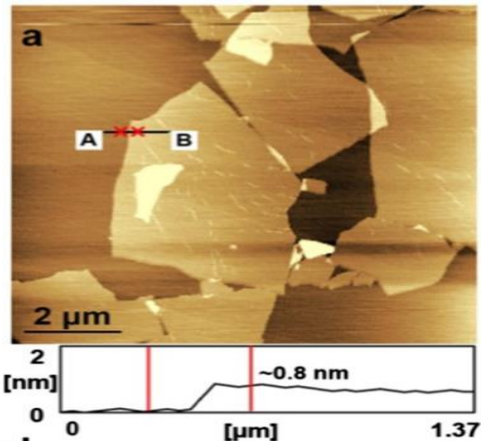

Fig 14. – (a) AFM-tapping mode of graphene produced by improved Hummers method.

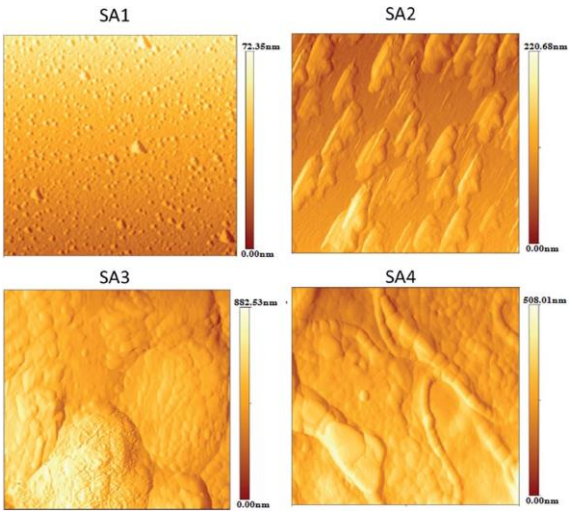

Fig 15. The images of AFM of SA1, 2, 3 and 4 gained in the sharp contact mode. (3*3 mm).

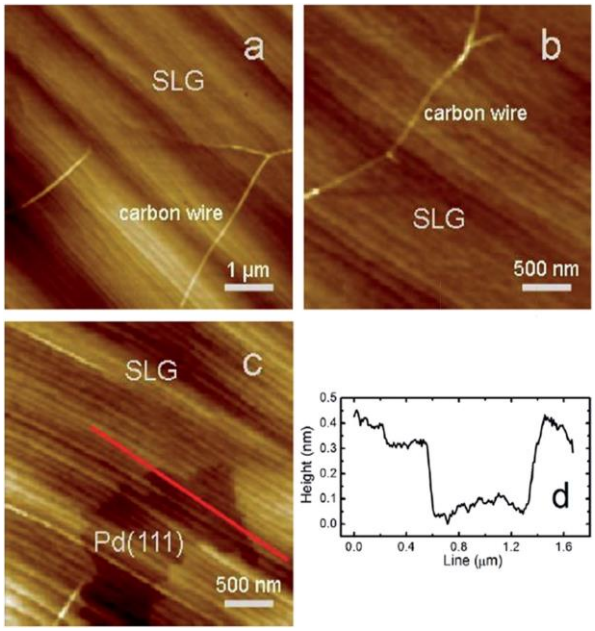

Fig 16. AFM graphene images which is formed on substrate of Pd111. Images (a and b) is from graphene sample center, Image (c) is from the graphene sample edge, image (d) shows the graphene layer height that refers to graphene (mono-layer).

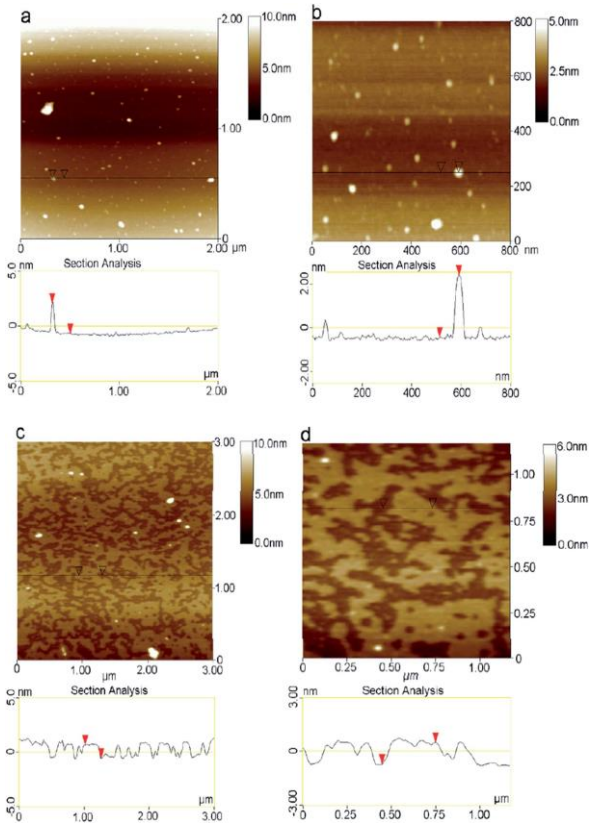

Fig 17. AFM graphene images of (a) multi-layer films (2 x 2 mm), (b) multi-layer of graphene films (0.8 x 0.8 mm), (c) single layer graphene films (3 x 3 mm), and (d) single layer of graphene films (1.25 x 1.25 mm).

3.5 UV-vis spectroscopy

UV-vis is an analysis to measures the radiation reflectance and absorption in the range of spectral UV. The molecules or atoms in the examined sample absorb the IR light, near UV, and visible regions throughout the electron's transitions. Also, the sample solution absorbance increased as the beam attenuation is increase. As reported by Beer's law [56-58], the absorbance relies on the solution concentration. UV-vis analysis is usually utilized to describe the graphene sheet optical transparency by determining the absorbance or transmittance properties of a sample [59]. A transmittance or absorption spectrum exhibits number of transmittance or absorption bands which refers to the electron transition from lowest to excited energy [60]. Hence, the UV-vis analysis might be successfully utilized to study the of graphene sheets properties [57].

UV-vis analysis can be implemented to show that graphite oxide has successfully decreased to decrease the graphene oxide [61]. Generally, the absorption peak of graphite-oxide is about 230 nm, which refers to transition of n-π* due to the existence of the C–C aromatic ring that reduced graphene oxide has an absorption peak shifted to 270 nm due to the transition of (n-π*) via bonds of carbonyl (C=O) [62,63], Figure 18. displays the reduced graphene oxide absorbance that is produced at different reaction times. It is found that the band of the sample that seen at 231 nm has clearly shifted to 270 nm as the time of reaction increase. The shifting of absorption peak beyond 270 nm, indicating that the process of graphite oxide reduction to of reduced graphene oxide has completed [64].

UV-vis analysis can be also employed to confirm the prepared graphene layers number. Figure 19(a). shows different peaks for the optical transmission from single to multi layers of graphene [65]. The increased layers number of prepared graphene decreases the optical transmission "an amount of light transmitted throughout a thick graphene sheet". As shown in Figure 19(a), the green curve refers to the barequartz transmission as the graphene sheet was placed. The wavelength number of all graphene samples have decreased from 250 nm to 300 nm and subsequently turn out to be linear after 600 nm [65].

Ago et al. [66] have also investigated the graphene sheet by estimating of the number of graphene layer based on the ratio of I_{2D} / I_G and the width of the band of 2D from Raman analysis is not precise or adequate as unanticipated doping could have happened in the graphene sheet in the mid of the transfer and growth processes. This unintended doping of graphene may change the I_{2D}/ I_G ratio and caused incorrect information being obtained on the graphene sheet quality. Furthermore, the band of 2D of double layer graphene can possess a narrow the width between 30 cm^{-1} and 40 cm^{-1} that is difficult to be detected and may mislead the approximation of the graphene layers number. Thus, Hiroki et al., employed UV-vis analysis to confirm that the converted-graphene is a graphene with single layer by determining the transmission of the light. It is found the optical transmission (550nm) was about 2.25%, this is in agreement with the theoretical value of graphene with a single layer, (2.3%). Therefore, the transferred layer is confirmed as a graphene (singlelayer) by UV-vis analysis. Also, Figure 19(b). exhibits the same value of optical-transmittance for the single layer synthesized by S. Bae et al. [67].

Graphene sheet is also a valuable material in optoelectronics and solar cells applications attributed to its high electrical-conductivity and good optical-transmittance that make this material a replacement of the presently utilized materials like fluorine tinoxide and indium tin-oxide. Dodoo-Arhin et al. [68] reported the excellent graphene characteristics by studying the differences of optical transmittance between transparent electrode and graphene. The optical transmittance of graphene at 97.7% is higher than the optical transmittance of the transparent electrode at 90.5%. Therefore, the light can easily pass

through graphene, these unique characteristics are important in photovoltaic applications.

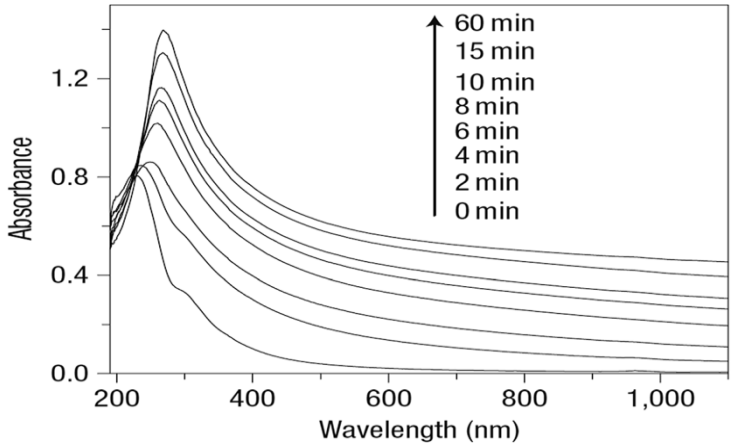

Fig 18. UV-vis spectra (absorption vs wavelength) presenting the variation of reduced graphene oxide as a reaction time function.

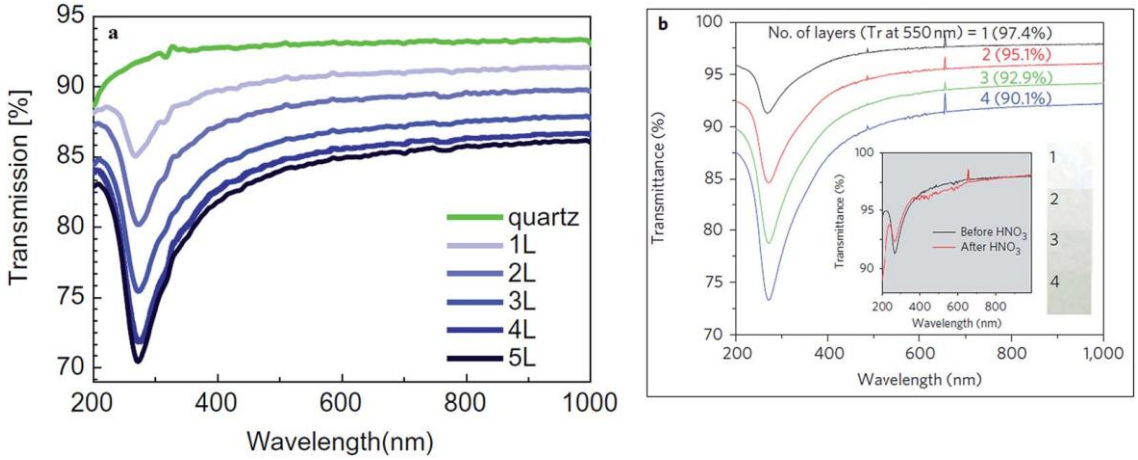

Fig 19. (a) UV-vis spectra (transmission vs wavelength) for bare-quartz and sheets of graphene on quartz.

5.5 XRD

XRD examination is utilized to investigate the crystal level of materials, size of crystallite, defects, atomic arrangement and other structural features. A material that has a crystalline structure is categorized via its orderly, arrangements of atoms planes [69]. XRD equipment are diffracted, scattered, refracted, absorbed, and transmitted [70]. A spectrum of diffraction is generated as X-rays are emitted from the equipment of XRD on a crystalline structure material.172 Moreover, the atoms planes separation of any material can be measured based on Bragg's law [69]. Same materials generate same spectra of XRD, thus an XRD analysis is considered as an essential reference to materials structure identification [71]. Each element in the mixture demonstrates different patterns of diffraction than other element. For graphene characterization, despite XRD analysis can be employed as a tool of characterization, it is not the perfect analysis used to describe the single layer graphene. However, XRD analysis still can be beneficial in assessing the structure of graphene.

Naebe et al. [72] have synthesized and investigated the reduced-graphene nanomaterial, which has higher thermal steadiness and better mechanical features than graphite oxide. The results of XRD exhibited reduced graphene, graphite oxide, graphite, and functionalized graphene, Figure. 20(a). The narrow diffraction curve of (2θ) at about 26 usually indicated the graphite (pristine) that is corresponding with the (002) plane atoms (well-ordered) of carbon with a spacing

(inter layer) of 3, 3 A˚. Though, the peak of graphite (well-ordered) at about 26 has vanished, whereas a low peak was observed at 2θ = 10 that suggests the (002) diffraction graphite oxide with a measured inter layer space at 8.5 A˚, which indicates that large quantities of oxygen atoms are attached the surface of the graphite oxide. Thus, the graphite oxide inter layer spacing is increased. The functional groups elimination, like an oxygen in the graphite oxide at a high temperature produced the peak disappearance of (002) and the developed the films of reduced graphene. Wang et al., [73] has also specified that the few layers of reduced graphene film has non-peak of (002) when the microwave irradiation conducted as shown in Figure 20(b).

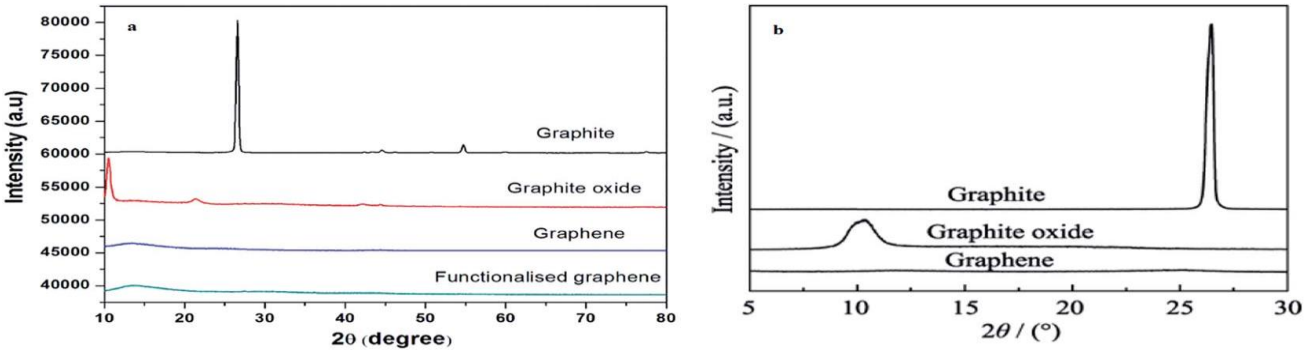

Fig 20. (a) XRD pattern for Functionalized Graphene, graphite, graphite oxide and graphene (b) XRD plots of graphene, graphite oxide, and natural graphite.

6. Conclusion

The graphene characterization has significantly developed and is now pushing the limit of characterization methods for nanomaterials, which will ease the understanding of nanomaterials and their developments towards several applications. Therefore, this work highlighted the most common methods used for graphene characterization. Based on the review and comparisons conducted on the related researches, it is found that the Raman-Spectroscopy is a significant technique for characterizing the thickness of graphene layer. Other methods will also offer as much evidence on the graphene structure as Raman spectroscopy, and any laboratory conducting a characterization of graphene without Raman would be considered as a disadvantage. SEM-FESEM, TEM and AFM are significantly applied to study the morphological properties of graphene by observing the morphological variations of the graphene sample. For a comprehensive study of graphene, XRD analysis can be also applied to understand the crystallinity aspects of the graphene.

References

[1] A. K. Geim and K. S. Novoselov, "The rise of graphene," *Nature Materials*, vol. 6, no. 3, pp. 183–191, Mar. 2007, doi: https://doi.org/10.1038/nmat1849.

[2] P. Avouris and C. Dimitrakopoulos, "Graphene: synthesis and applications," *Materials Today*, vol. 15, no. 3, pp. 86–97, Mar. 2012, doi: https://doi.org/10.1016/s1369-7021(12)70044-5.

[3] B. Luo, S. Liu, and L. Zhi, "Chemical Approaches toward Graphene-Based Nanomaterials and their Applications in Energy-Related Areas," *Small*, vol. 8, no. 5, pp. 630–646, Nov. 2011, doi: https://doi.org/10.1002/smll.201101396.

[4] C. N. R. Rao, A. K. Sood, K. S. Subrahmanyam, and A. Govindaraj, "Graphene: The New Two-Dimensional Nanomaterial," *Angewandte Chemie International Edition*, vol. 48, no. 42, pp. 7752–7777, Oct. 2009, doi: https://doi.org/10.1002/anie.200901678.

[5] J. Liu, L. Cui, D. Losic, Graphene and graphene oxide as new nanocarriers for drug delivery applications, Acta Biomater. 9 (2013) 9243–9257, http://dx.doi. org/10.1016/j.actbio.2013.08.016.

[6] E. Quesnel et al., "Graphene-based technologies for energy applications, challenges and perspectives," vol. 2, no. 3, pp. 030204–030204, Aug. 2015, doi: https://doi.org/10.1088/2053-1583/2/3/030204.

[7] S. P. Surwade *et al.*, "Water desalination using nanoporous single-layer graphene," *Nature*

Nanotechnology, vol. 10, no. 5, pp. 459–464, May 2015, doi: https://doi.org/10.1038/nnano.2015.37.

[8] K. Yang, L. Feng, and Z. Liu, "Stimuli responsive drug delivery systems based on nano-graphene for cancer therapy," *Advanced Drug Delivery Reviews*, vol. 105, pp. 228–241, Oct. 2016, doi: https://doi.org/10.1016/j.addr.2016.05.015.

[9] M. Núñez-Regueiro, "Yaşlı Kadınlarda Üreme Sağlığı," *DergiPark (Istanbul University)*, vol. 1, no. 1, Feb. 2015, doi: https://doi.org/10.1016/j.

[10] B. Marinho, M. Ghislandi, E. Tkalya, C. E. Koning, and G. de With, "Electrical conductivity of compacts of graphene, multi-wall carbon nanotubes, carbon black, and graphite powder," *Powder Technology*, vol. 221, pp. 351–358, May 2012, doi: https://doi.org/10.1016/j.powtec.2012.01.024.

[11] M. Amoretti *et al.*, "Production and detection of cold antihydrogen atoms," *Nature*, vol. 419, no. 6906, pp. 456–459, Oct. 2002, doi: https://doi.org/10.1038/nature01096.

[12] R. K. Joshi, S. Alwarappan, M. Yoshimura, V. Sahajwalla, and Y. Nishina, "Graphene oxide: the new membrane material," *Applied Materials Today*, vol. 1, no. 1, pp. 1–12, Nov. 2015, doi: https://doi.org/10.1016/j.apmt.2015.06.002.

[13] Y. Song, Y. Luo, C. Zhu, H. Li, D. Du, and Y. Lin, "Recent advances in electrochemical biosensors based on graphene two-dimensional nanomaterials," *Biosensors and Bioelectronics*, vol. 76, pp. 195–212, Feb. 2016, doi: https://doi.org/10.1016/j.bios.2015.07.002.

[14] E. O. Polat, H. B. Uzlu, O. Balci, N. Kakenov, E. Kovalska, and C. Kocabas, "Graphene-Enabled Optoelectronics on Paper," *ACS Photonics*, vol. 3, no. 6, pp. 964–971, Jun. 2016, doi: https://doi.org/10.1021/acsphotonics.6b00017.

[15] X. Wang, W. Xie, and J.-B. Xu, "Graphene Based Non-Volatile Memory Devices," *Advanced Materials*, vol. 26, no. 31, pp. 5496–5503, Feb. 2014, doi: https://doi.org/10.1002/adma.201306041.

[16] Q. Ke and J. Wang, "Graphene-based materials for supercapacitor electrodes – A review," *Journal of Materiomics*, vol. 2, no. 1, pp. 37–54, Mar. 2016, doi: https://doi.org/10.1016/j.jmat.2016.01.001.

[17] F. Schwierz, "Graphene transistors," *Nature Nanotechnology*, vol. 5, no. 7, pp. 487–496, May 2010, doi: https://doi.org/10.1038/nnano.2010.89.

[18] F. Withers *et al.*, "Light-emitting diodes by band-structure engineering in van der Waals heterostructures," *Nature Materials*, vol. 14, no. 3, pp. 301–306, Mar. 2015, doi: https://doi.org/10.1038/nmat4205.

[19] H.-J. Choi, S.-M. Jung, Jeong Gil Seo, Dong Kyung Chang, L. Dai, and J.-B. Baek, "Graphene for energy conversion and storage in fuel cells and supercapacitors," *Nano Energy*, vol. 1, no. 4, pp. 534–551, Jul. 2012, doi: https://doi.org/10.1016/j.nanoen.2012.05.001.

[20] K. J. Tielrooij *et al.*, "Photoexcitation cascade and multiple hot-carrier generation in graphene," *Nature Physics*, vol. 9, no. 4, pp. 248–252, Feb. 2013, doi: https://doi.org/10.1038/nphys2564.

[21] S. S. Gupta, T. S. Sreeprasad, S. M. Maliyekkal, S. K. Das, and T. Pradeep, "Graphene from Sugar and its Application in Water Purification," *ACS Applied Materials & Interfaces*, vol. 4, no. 8, pp. 4156–4163, Jul. 2012, doi: https://doi.org/10.1021/am300889u.

[22] G. Wang, X. Shen, J. Yao, and J. Park, "Graphene nanosheets for enhanced lithium storage in lithium ion batteries," *Carbon*, vol. 47, no. 8, pp. 2049–2053, Jul. 2009, doi: https://doi.org/10.1016/j.carbon.2009.03.053.

[23] Y. Wu, T. Yu, and Z.-X. Shen, "Two-dimensional carbon nanostructures: Fundamental properties, synthesis, characterization, and potential applications," vol. 108, no. 7, pp. 071301–071301, Oct. 2010, doi: https://doi.org/10.1063/1.3460809.

[24]. A. J. Van Bommel, J. E. Crombeen, and A. Van Tooren, "LEED and Auger electron observations of the SiC(0001) surface," *Surface Science*, vol. 48, no. 2, pp. 463–472, Mar. 1975, doi: https://doi.org/10.1016/0039-6028(75)90419-7.

[25] De Heer W., The development of epitaxial graphene for 21st century electronics; ar Xiv: 1012. 1644v1.

[26] W. A. de Heer *et al.*, "Large area and structured epitaxial graphene produced by confinement controlled sublimation of silicon carbide," *Proceedings of the National Academy of Sciences*, vol. 108, no. 41, pp. 16900–16905, Sep. 2011, doi: https:// doi.org/10.1073/pnas.1105113108.

[27] J. Hass *et al.*, "Highly ordered graphene for two dimensional electronics," *Applied Physics Letters*, vol. 89, no. 14, p. 143106, Oct. 2006, doi: https://doi.org/10.1063/1.2358299.

[28] Hass, J., Milla´n-Otoya, J.E., First, P.N., Conrad, E.H.: Interface structure of epitaxial graphene grown on 4H-SiC(0001). Phys Rev B 78, 205424 (2008). doi:10.1103/PhysRevB.78.205424

[29] C. Berger *et al.*, "Ultrathin Epitaxial Graphite: 2D Electron Gas Properties and a Route toward Graphene-based Nanoelectronics," *The Journal of Physical Chemistry B*, vol. 108, no. 52, pp. 19912–19916, Dec. 2004, doi: https://doi.org/10.1021/jp040650f.

[30] I. Forbeaux, J.-M. Themlin, A. Charrier, F. Thibaudau, and J.-M. Debever, "Solid-state graphitization mechanisms of silicon carbide 6H–SiC polar faces," *Applied Surface Science*, vol. 162–163, pp. 406–412, Aug. 2000, doi: https://doi.org/10.1016/s0169-4332(00)00224-5.

[31] J. Hass *et al.*, "Highly ordered graphene for two dimensional electronics," *Applied Physics Letters*, vol. 89, no. 14, p. 143106, Oct. 2006, doi: https://doi.org/10.1063/1.2358299.

[32] A. Reina *et al.*, "Large Area, Few-Layer Graphene Films on Arbitrary Substrates by Chemical Vapor Deposition," *Nano Letters*, vol. 9, no. 1, pp. 30–35, Jan. 2009, doi: https://doi.org/10.1021/nl801827v.

[36] K. S. Kim *et al.*, "Large-scale pattern growth of graphene films for stretchable transparent electrodes," *Nature*, vol. 457, no. 7230, pp. 706–710, Jan. 2009, doi: https://doi.org/10.1038/nature07719.

[37] X. Li *et al.*, "Large-Area Synthesis of High-Quality and Uniform Graphene Films on Copper Foils," *Science*, vol. 324, no. 5932, pp. 1312–1314, May 2009, doi: https://doi.org/10.1126/science.1171245.

[38] Q. Wang, X. Wang, Z. Chai, and W. Hu, "Low-temperature plasma synthesis of carbon nanotubes and graphene based materials and their fuel cell applications," *Chemical Society Reviews*, vol. 42, no. 23, p. 8821, 2013, doi: https://doi.org/10.1039/c3cs60205b.

[39] V. H. Pham *et al.*, "One-step synthesis of superior dispersion of chemically converted graphene in organic solvents," *Chemical Communications*, vol. 46, no. 24, p. 4375, 2010, doi: https://doi.org/10.1039/c0cc00363h.

[40] S. Guo, S. Dong, and E. Wang, "Three-Dimensional Pt-on-Pd Bimetallic Nanodendrites Supported on Graphene Nanosheet: Facile Synthesis and Used as an Advanced Nanoelectrocatalyst for Methanol Oxidation," *ACS Nano*, vol. 4, no. 1, pp. 547–555, Dec. 2009, doi: https://doi.org/10.1021/nn9014483.

[41] X. Wang *et al.*, "Large-Scale Synthesis of Few-Layered Graphene using CVD," *Chemical Vapor Deposition*, vol. 15, no. 1–3, pp. 53–56, Mar. 2009, doi: https://doi.org/10.1002/cvde.200806737.

[42] K. V. Emtsev, F. Speck, T. Seyller, L. Ley, and J. G. Riley, "Interaction, growth, and ordering of epitaxial graphene on SiC{0001} surfaces: A comparative photoelectron spectroscopy study," *Physical Review B*, vol. 77, no. 15, Apr. 2008, doi: https://doi.org/10.1103/physrevb.77.155303.

[43] L. S. Panchakarla, A. Govindaraj, and R. Rao, "Boron- and nitrogen-doped carbon nanotubes and graphene," *Inorganica Chimica Acta*, vol. 363, no. 15, pp. 4163–4174, Dec. 2010, doi: https://doi.org/10.1016/j.ica.2010.07.057.

[44] Y.-M. . Lin *et al.*, "100-GHz Transistors from Wafer-Scale Epitaxial Graphene," *Science*, vol. 327, no. 5966, pp. 662–662, Feb. 2010, doi: https://doi.org/10.1126/science.1184289.

[45] K. S. Novoselov *et al.*, "Two-dimensional gas of massless Dirac fermions in graphene," *Nature*, vol. 438, no. 7065, pp. 197–200, 2005, doi: https://doi.org/10.1038/nature04233.

[46] X. Chen, L. Zhang, and S. Chen, "Large area CVD growth of graphene," *Synthetic Metals*, vol. 210, pp. 95–108, Dec. 2015, doi: https://doi.org/10.1016/j.synthmet.2015.07.005.

[47] Liu, Zhongfan, Li Lin, Huaying Ren, and Xiao Sun. "CVD synthesis of graphene." In Thermal transport in carbon-based nanomaterials, pp. 19-56. Elsevier, 2017.

[48] D. Fray, A. Kamali, Method of Producing Graphene, Google Patents, 2017.

[49] A. Wu, X. Li, J. Yang, C. Du, W. Shen, and J. Yan, "Upcycling Waste Lard Oil into Vertical Graphene Sheets by Inductively Coupled Plasma Assisted Chemical Vapor Deposition," *Nanomaterials*, vol. 7, no. 10, p. 318, Oct. 2017, doi: https://doi.org/10.3390/nano7100318.

[50] Bo, Zheng, Mu Yuan, Shun Mao, Xia Chen, Jianhua Yan, and Kefa Cen. "Decoration of vertical graphene with tin dioxide nanoparticles for highly sensitive room temperature formaldehyde sensing." *Sensors and Actuators B: Chemical* 256 (2018): 1011-1020.

[51] K. Krishnamoorthy, G.-S. Kim, and S. J. Kim, "Graphene nanosheets: Ultrasound assisted synthesis and characterization," *Ultrasonics Sonochemistry*, vol. 20, no. 2, pp. 644–649, Mar. 2013, doi: https://doi.org/10.1016/j.ultsonch.2012.09.007.

[52] V. Abdelsayed, S. Moussa, Hassan M.A. Hassan, Hema Aluri, M. M. Collinson, and M. Samy El-Shall, "Photothermal Deoxygenation of Graphite Oxide with Laser Excitation in Solution and Graphene-Aided

Increase in Water Temperature," *The Journal of Physical Chemistry Letters*, vol. 1, no. 19, pp. 2804–2809, Sep. 2010, doi: https://doi.org/10.1021/jz1011143.

[53] Y. Zhou *et al.*, "Microstructuring of Graphene Oxide Nanosheets Using Direct Laser Writing," *Advanced Materials*, vol. 22, no. 1, pp. 67–71, Jan. 2010, doi: https://doi.org/10.1002/adma.200901942.

[54] J. Chen, B. Yao, C. Li, and G. Shi, "An improved Hummers method for eco-friendly synthesis of graphene oxide," *Carbon*, vol. 64, pp. 225–229, Nov. 2013, doi: https://doi.org/10.1016/j.carbon.2013.07.055.

[55] C. Liu, G. Hu, and H. Gao, "Preparation of few-layer and single-layer graphene by exfoliation of expandable graphite in supercritical N,N-dimethylformamide," *The Journal of Supercritical Fluids*, vol. 63, pp. 99–104, Mar. 2012, doi: https://doi.org/10.1016/j.supflu.2012.01.002.

[56] S. Bae *et al.*, "Roll-to-roll production of 30-inch graphene films for transparent electrodes," *Nature nanotechnology*, vol. 5, no. 8, pp. 574–8, 2010, doi: https://doi.org/10.1038/nnano.2010.132.

[57] Ved Prakash Verma, S. Das, I. Lahiri, and W. Choi, "Large-area graphene on polymer film for flexible and transparent anode in field emission device," *Applied Physics Letters*, vol. 96, no. 20, pp. 203108–203108, May 2010, doi: https://doi.org/10.1063/1.3431630.

[58] Chen, Z.H., Lin, Y.M., Rooks, M.J., Avouris, P.: Graphene nano-ribbon electronics. Phys. E-Low-Dimens. Syst. Nanos- tructures 40(2), 228–232 (2007). doi:10.1016/j.physe.2007.06. 020

[59] D. B. Shinde, J. Debgupta, A. Kushwaha, M. Aslam, and V. K. Pillai, "Electrochemical Unzipping of Multi-walled Carbon Nanotubes for Facile Synthesis of High-Quality Graphene Nanoribbons," *Journal of the American Chemical Society*, vol. 133, no. 12, pp. 4168–4171, Mar. 2011, doi: https://doi.org/10.1021/ja1101739.

[60] A. G. Cano-Márquez *et al.*, "Ex-MWNTs: Graphene Sheets and Ribbons Produced by Lithium Intercalation and Exfoliation of Carbon Nanotubes," *Nano Letters*, vol. 9, no. 4, pp. 1527–1533, Mar. 2009, doi: https://doi.org/10.1021/nl803585s.

[61] L. Jiao, X. Wang, G. Diankov, H. Wang, and H. Dai, "Facile synthesis of high-quality graphene nanoribbons," *Nature Nanotechnology*, vol. 5, no. 5, pp. 321–325, Apr. 2010, doi: https://doi.org/10.1038/nnano.2010.54.

[62] L. Jiao, L. Zhang, X. Wang, G. Diankov, and H. Dai, "Narrow graphene nanoribbons from carbon nanotubes," *Nature*, vol. 458, pp. 877–880, Apr. 2009, doi: https://doi.org/10.1038/nature07919.

[63] Krane, N. (2011). Preparation of graphene. *Selected topics in physics: physics of nanoscale carbon*, 872-876.

[64] Z.-S. Wu *et al.*, "Synthesis of Graphene Sheets with High Electrical Conductivity and Good Thermal Stability by Hydrogen Arc Discharge Exfoliation," *ACS Nano*, vol. 3, no. 2, pp. 411–417, Feb. 2009, doi: https://doi.org/10.1021/nn900020u.

[65] Z. Wang, N. Li, Z. Shi, and Z. Gu, "Low-cost and large-scale synthesis of graphene nanosheets by arc discharge in air," *Nanotechnology*, vol. 21, no. 17, p. 175602, Apr. 2010, doi: https://doi.org/10.1088/0957-4484/21/17/175602.

[66] N. Li, Z. Wang, K. Zhao, Z. Shi, Z. Gu, and S. Xu, "Large scale synthesis of N-doped multi-layered graphene sheets by simple arc-discharge method," *Carbon*, vol. 48, no. 1, pp. 255–259, Jan. 2010, doi: https://doi.org/10.1016/j.carbon.2009.09.013.

[67] V. C. Tung, M. J. Allen, Y. Yang, and R. B. Kaner, "High-throughput solution processing of large-scale graphene," *Nature Nanotechnology*, vol. 4, no. 1, pp. 25–29, Nov. 2008, doi: https://doi.org/10.1038/nnano.2008.329.

[68] J. Chen, L. Chen, Z. Zhang, J. Li, L. Wang, and W. Jiang, "Graphene layers produced from carbon nanotubes by friction," *Carbon*, vol. 50, no. 5, pp. 1934–1941, Apr. 2012, doi: https://doi.org/10.1016/j.carbon.2011.12.044.

[69] A. Gedanken, "Using sonochemistry for the fabrication of nanomaterials," *Ultrasonics Sonochemistry*, vol. 11, no. 2, pp. 47–55, Apr. 2004, doi: https://doi.org/10.1016/j.ultsonch.2004.01.037.

[70] M. Veerapandian, S. Sadhasivam, J. Choi, and K. Yun, "Glucosamine functionalized copper nanoparticles: Preparation, characterization and enhancement of anti-bacterial activity by ultraviolet irradiation," *Chemical Engineering Journal*, vol. 209, pp. 558–567, Oct. 2012, doi: https://doi.org/10.1016/j.cej.2012.08.054.

[72] C. Deng, H. Hu, X. Ge, C. Han, D. Zhao, and G. Shao, "One-pot sonochemical fabrication of hierarchical hollow CuO submicrospheres," vol. 18, no. 5, pp. 932–937, Sep. 2011, doi: https://doi.org/10.1016/j.ultsonch.2011.01.007.

[71] D. V. Pinjari and A. B. Pandit, "Room temperature synthesis of crystalline CeO2 nanopowder: Advantage of sonochemical method over conventional method,"

Ultrasonics Sonochemistry, vol. 18, no. 5, pp. 1118–1123, Sep. 2011, doi: https://doi.org/10.1016/j.ultsonch.2011.01.008.

[72] V. Safarifard and A. Morsali, "Sonochemical syntheses of a nano-sized copper (II) supramolecule as a precursor for the synthesis of copper (II) oxide nanoparticles," *Ultrasonics Sonochemistry*, vol. 19, no. 4, pp. 823–829, Jul. 2012, doi: https://doi.org/10.1016/j.ultsonch.2011.12.013.

[73] A. Ramadoss and S. J. Kim, "Synthesis and characterization of HfO2 nanoparticles by sonochemical approach," *Journal of Alloys and Compounds*, vol. 544, pp. 115–119, Dec. 2012, doi: https://doi.org/10.1016/j.jallcom.2012.08.005.